Journal Title: Tectonophysics
Volume: 225
Issue: 4
Month/Year: 19931030
Pages: 529-542

Article Author: Dasgupta, Sujit
Article Title: Seismicity and plate deformation below the Andaman Arc, northeastern Indian Ocean

Tectonophysics, 225 (1993) 529–542
Elsevier Science Publishers B.V., Amsterdam

Seismicity and plate deformation below the Andaman arc, northeastern Indian Ocean

Sujit Dasgupta [a] and Manoj Mukhopadhyay [b]*

[a] *Publication Division, Geological Survey of India, 29, J.L. Nehru Road, Calcutta-700016, India*
[b] *Department of Geophysics, Indian School of Mines, Dhanbad-826004, India*

(Received January 20, 1992; revised version accepted March 18, 1993)

ABSTRACT

The seismic activity originating below the Andaman arc–Sea region is generally discernible into fore- and back-arc seismic zones which are traceable for nearly 1500 km in a N–S direction at the junctures between the Indian, Burma and SE Asia plates. The fore-arc seismicity displays an east-dipping (40–55°) Benioff zone upto about 200 km focal depths. Details of the Benioff zone, in correspondence to the observed gravity field, are discussed in four N–S sectors, which suggest some significant variations in the configuration of the Benioff zone. The back-arc seismicity affects only the top 40–45 km of the lithosphere below the Andaman Sea, where the back-arc spreading ridge splits the volcanic arc. Stress distribution and faulting due to earthquakes below the Andaman–West Sunda arc are studied here using 68 focal mechanism solutions. Their most significant results are: low-angle thrust events occur along the upper edge of the descending Indian plate, downdip tensional events have steeply dipping ($\geq 60°$) nodal planes, and normal faulting takes place in most parts of the Benioff zone along moderately dipping (30–45°) planes. Downdip compressional events (high-angle reverse fault, nodal plane dip $> 60°$) or reverse faulting along moderately dipping (30–45°) nodal planes also occur below the Andaman arc. The compressive earthquakes dominate the shallower level of the subducting slab, and the tensional stress observed locally in north part of the Andaman Sea may be an outcome of the weak coupling between the descending and overriding plates. Generally, a more or less complete sequence of faulting, i.e., thrusting below the trench, normal faulting below the fore arc, and strike-slip motion along the inner edges of the fore arc characterize the Andaman–West Sunda arc. In the southern Andaman region, a rather oblique convergence between the Indian Ocean and the SE Asia plates is needed to explain the existence of a somewhat contorted Benioff zone, in which, compressional stress dominates in deeper lithosphere. Oceanward, the Ninetyeast Ridge also impinges on the subduction zone in this region. Left-lateral shear motion along the east margin of the Ninetyeast Ridge is further inferred by the results of focal mechanism solutions.

Introduction

The Andaman–Nicobar–Nias sedimentary island arc in the northeastern Indian Ocean defines a nearly 2200-km-long "trench slope break" between the Indian plate and the SE Asia/Burma plate (Curray et al., 1979). This convergent margin joins the Burmese arc to the north and links with the Sunda arc towards the south (Fig. 1). Active subduction of the Indian lithosphere below the Burma plate is primarily documented by the presence of: (1) the Barren–Narcondam active volcanic arc (the Barren last erupted in June 1991) that continues to the continental margin arc in Sumatra (Rodolfo, 1969; Fig. 2); (2) an east-dipping Benioff zone defined by earthquakes upto 200 km focal depth (Mukhopadhyay, 1984); (3) an anomalous heat-flow pattern (Closs et al., 1974; Curray et al., 1982); and (4) by a large-amplitude bipolar gravity field characteristic of subduction zones (Mukhopadhyay, 1988; Mukhopadhyay and Krishna, 1991). The geological and tectonic history of the region is complex due to the presence of active faults/tectonic features such as the West Andaman fault in the Andaman arc, the Semangko fault in Sumatra, the Sagaing right-lateral transform in Burma, and the Neogene Andaman back-arc spreading ridge between

* Present address: The Petroleum Centre, NTH, 7034 Trondheim, Norway.

the trench slope from the Andaman and Sunda arc regions (Moore and Curray, 1980; Moore and Karig, 1980; Moore et al., 1980; Curray et al.,

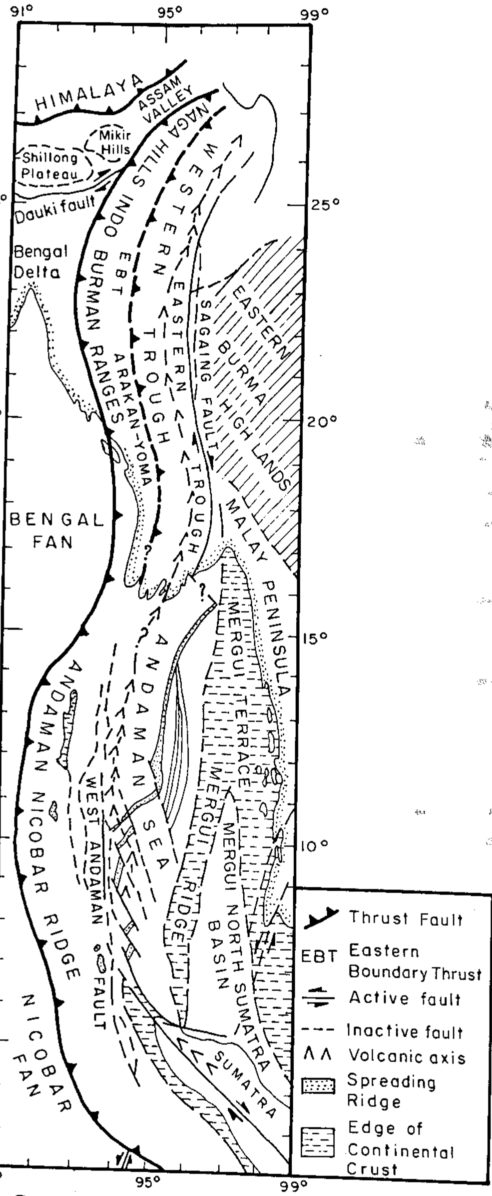

Fig. 1. Generalized tectonic map of the northeastern Indian Ocean showing the continuity of the Andaman arc into Burma and Sumatra (after Curray et al., 1979).

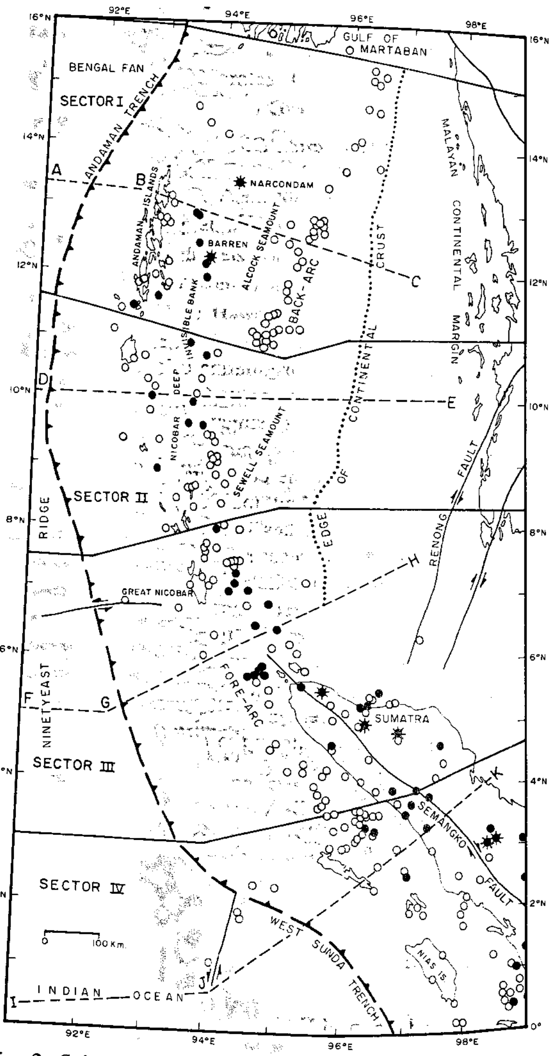

Fig. 2. Seismicity map for the Andaman–West Sunda arc. Earthquake data sampling period: 1964–1984; data source ISC bulletin; ○ = focal depth (h) $\leqslant 70$ km; ● = $h > 70$ km. The study area is classified into four sectors, I–IV, in accordance with the change in strike of the trench–slope break, gravity anomaly trend, and seismicity cluster/lineaments. All earthquake events with $m_b \geqslant 4.9$ are plotted in sectors I and II; in sectors III and IV $m_b \geqslant 5.0$ and $m_b \geqslant 4.9$ for events with $h \geqslant 70$ km and $h \leqslant 70$ km, respectively. The dashed line with solid teeth marks the subduction zone; star symbol is for sub-Recent/Recent volcano. A pronounced gravity minimum occurs farther east mostly over the fore-arc in sectors III and IV and below the Nicobar deep in Sector II. Sections *ABC* through *IJK* taken in mid-part of individual sectors are illustrated in Fig. 3.

them. The latter is related to oblique convergence of the Indian plate against the Asian continental margin; actual spreading occurred possibly through leaky transform (Uyeda and Kanamori, 1979). The Andaman basin underlying the greater part of the Andaman Sea is categorized as a "pull-apart" or "rip-off" basin (Curray, 1987; Maung, 1987), rather than a typical back-arc extensional basin. Seismic reflection studies across

1982) indicate folding and thrusting in the accretionary prism, where a major component of convergence occurs normal to the trench axis (Curray, 1987).

Here we use earthquake data to study details of the Andaman–West Sunda arc subduction zone over its various segments for a distance of about 1500 km in a N–S direction. Stress distribution and fault pattern in the Benioff zone are examined using a large number of focal mechanism solutions. Tectonic trends, gravity anomaly zones and results obtained from the analysis of earthquake focal mechanism solutions are synthesized from the viewpoint of stress distribution, Benioff zone configuration, plate deformation and tectonics of the Andaman–West Sunda arc.

Seismicity below the Andaman arc–Sea region

The seismicity map for the Andaman arc–Sea region for the period 1964–1984 (data source: ISC Bull.) is shown in Figure 2, where, events of $m_b \geqslant 4.9$ are plotted. In order to study the details of the seismicity, the following four sectors are defined in the figure based on morphotectonic setting, gravity anomaly trends (after Mukhopadhyay, 1988) and seismicity patterns:

Sector I corresponding to the NNE-trending Andaman arc where the Narcondam and Barren volcanic islands represent an intraoceanic magmatic arc within a fore-arc setting; the Alcock Seamount further divides the Andaman Sea into fore- and back-arc basins.

In Sector II the major bathymetric and structural features are the Nicobar Deep lying to the east of the Little Andaman–Car Nicobar islands (Rodolfo, 1969). The Sewell Seamount in this sector occupies a position identical to that of the Alcock Seamount in Sector I; both seamounts represent the pre-Miocene magmatic arc. The NinetyeastRidge is obliquely oriented to the Andaman trench. At about 10°N, the ridge even locally abuts against the trench.

Sector III corresponds to the Great Nicobar Islands and northern Sumatra, where the Indian, Burma and SE Asia plates meet.

Orientation of the fore arc gradually changes to WNW–ESE in Sector IV, where it is represented by the Simelue and Nias islands of offshore Sumatra. Here, the fore-arc basin and the magmatic arc are closely associated with the Semangko fault.

For each of these sectors we present representative sections for free-air gravity, bathymetry and earthquake hypocentre distribution profiles ABC, DE, FGH and IJK in Figures 2 and 3.

For each sector, orientation of the section was chosen to give true attitudes of the lithospheric plates in a single profile taking into consideration the morphotectonic, gravity and seismicity pattern. In preparing the Benioff zone sections, the earthquake events located within individual sectors were projected onto a vertical plane underlying each of the profiles. As can be seen from Figure 3, an inclined seismic zone is common to all the sectors, with, however, variable density of seismic incidence and depth of penetration within the asthenosphere. Earthquake foci range in depth from near surface to around 180 km. The foci distribution in the inclined seismic zone is used to define boundaries of the subducting Indian plate below the Andaman–Sunda arc. The horizontal lower boundary of the plate is placed at about 80 km depth in all the sectors based on the hypocentral distribution in the initial flexure region of the slab. When traced eastward, the seismic slab dips to the east and the initial flexural bending occurs in the region of the fore arc. Depth of penetration of the slab increases from north to south, varying from about 160 km in sectors I and II, through 180 km in Sector III, and 200 km in Sector IV. The dip of the Benioff zone varies from 55° eastward in Sector I to 40–45° in sectors II through IV. Further east of the Benioff zone occurs an inland seismic slab defining the western edge of the Burma plate. A relatively shallow seismic zone occurs in Sector I below the Andaman Sea which clearly represents the back-arc seismicity related to spreading of the Burma plate. In Sector III, no such back-arc activity is observed, instead, there is a cluster of shallow seismic events in the vicinity of the Benioff zone below the Nicobar Deep and a somewhat contorted Benioff zone further east at the Malayan margin. It will be discussed in a subsequent section that the stress and fault pattern are quite different in the Andaman back-arc and Nicobar Deep; the latter is a modified fore-arc trough. The inclined seismic slab at shallow level is much diffused in sectors III and IV, which makes it difficult to delineate the upper boundary of the Benioff zone on the basis of the rather poorly defined inland seismic slab alone. This is more so since the seismicity within the inland slab usually restricts to the fore-arc–magmatic arc region. At least part of this seismic acitivity must be

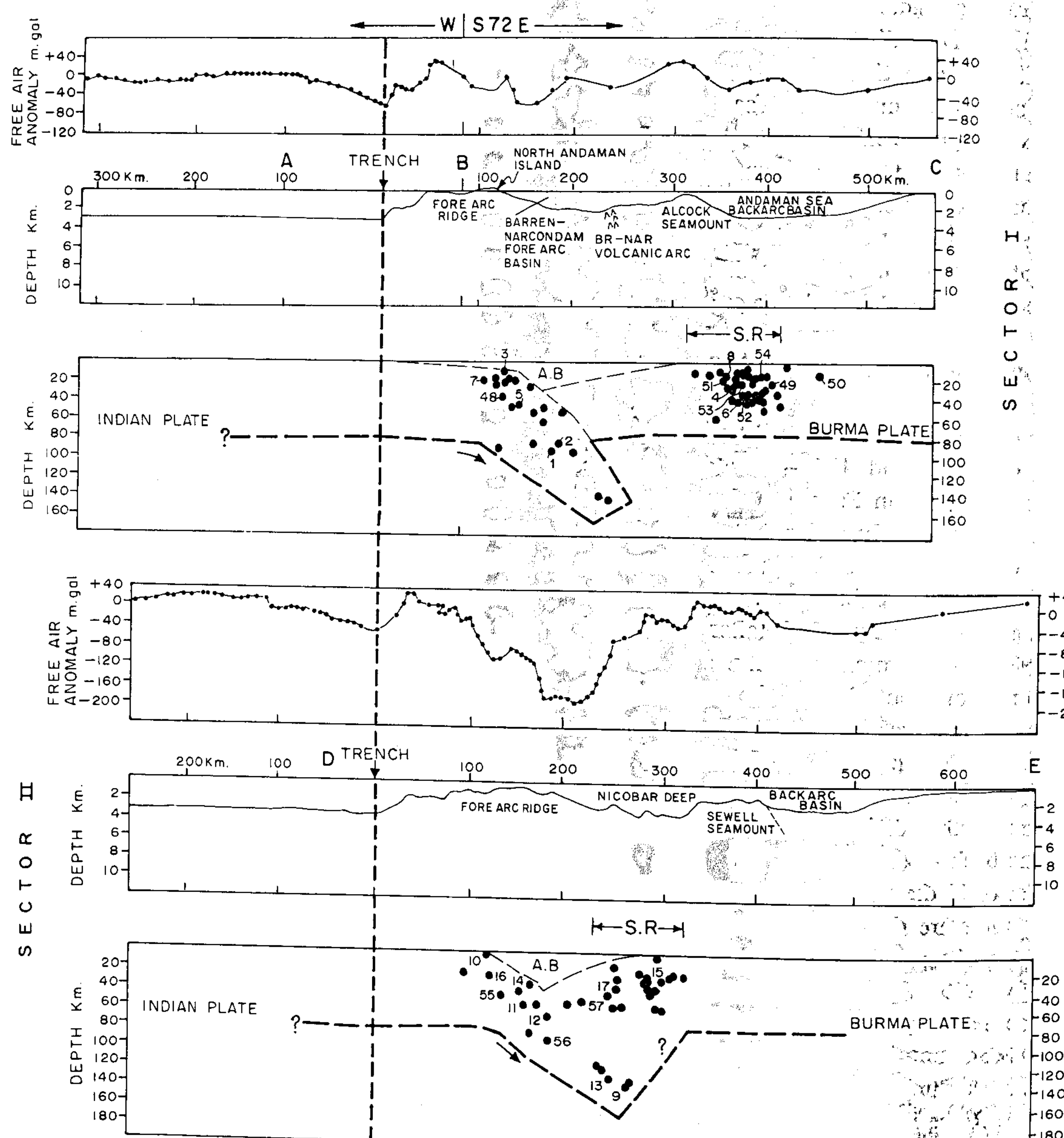

Fig. 3. Sections *ABC* through *IJK* between northern Andaman and central Sumatra (Fig. 2 for location) illustrate gravity anomaly, bathymetry and related morphotectonic elements, and underlying seismic zones. The westernmost gravity-bathymetry low defines the probable trench location east of which the Benioff zone starts developing. *A.B.* is a triangular aseismic belt between the subducting Indian plate and the overriding Burma plate. A gravity minimum outlines the Aseismic Belt that correlates to the Nicobar Deep in sectors I and II (a) but it shifts further seaward in sectors III and IV (b). *C.B.Z.* refers to Contorted Benioff zone in southern Andaman–northern Sumatra; *S.R.* approximates the location of the Andaman Spreading Ridge. Digits refer to focal mechanism solutions listed in Table 1 and plotted (new solutions) in Fig. 4.

originating in relation to the Semangko fault. The inland seismic slab within the Burma plate extends down to about 60 km. A triangular aseismic belt is described by the upper surfaces of the Benioff zone and the inland seismic slab in all four sectors, though this is not equally pronounced everywhere. The apex of the aseismic belt is always deflected downwards, concordant with the dip of the Benioff zone; this is presumably a consequence of the loading by the accretionary wedge near the subduction zone. Further, the apex of the Benioff zone locates seaward of the fore-arc basin in sectors I and II, whereas it is more landward in sectors III and IV.

Stress distribution and fault pattern below the Andaman arc–Sea region

Here we consider 68 focal mechanism solutions for both shallow and intermediate earth-

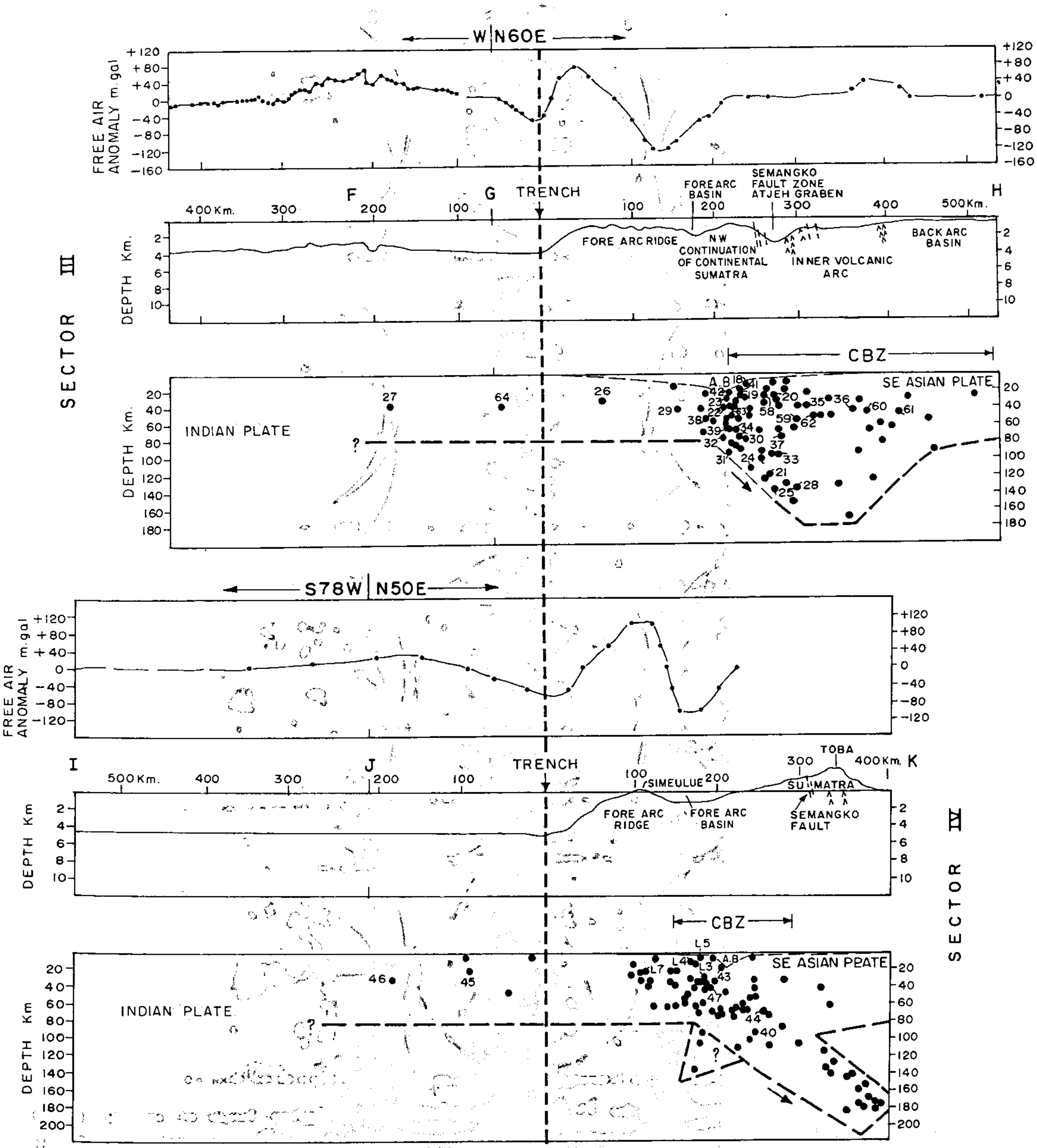

Fig. 3 (continued)

quakes in the Andaman–West Sunda arc for studying the stress distribution and faulting pattern. Of these, 47 solutions are new while the rest is taken from published solutions. Of these, at least 34 events relate to the Benioff zone seismicity. The new focal mechanism solutions are shown in Figure 4, and their parameters are listed in Table 1. The solution results are schematically represented on Figure 5.

Figures 4 and 5, and Table 1 demonstrate that four distinct categories of faulting and stress pattern characterize the subducting Indian plate below the Andaman–West Sunda arc region. They are:

(1) Low-angle thrust events in the descending plate as evidenced by solutions 2 and 7 in Sector I, 9, 11 and 12 in Sector II, 41 and 63 in Sector III, and L4, L7 (both after Newcomb and Mc-

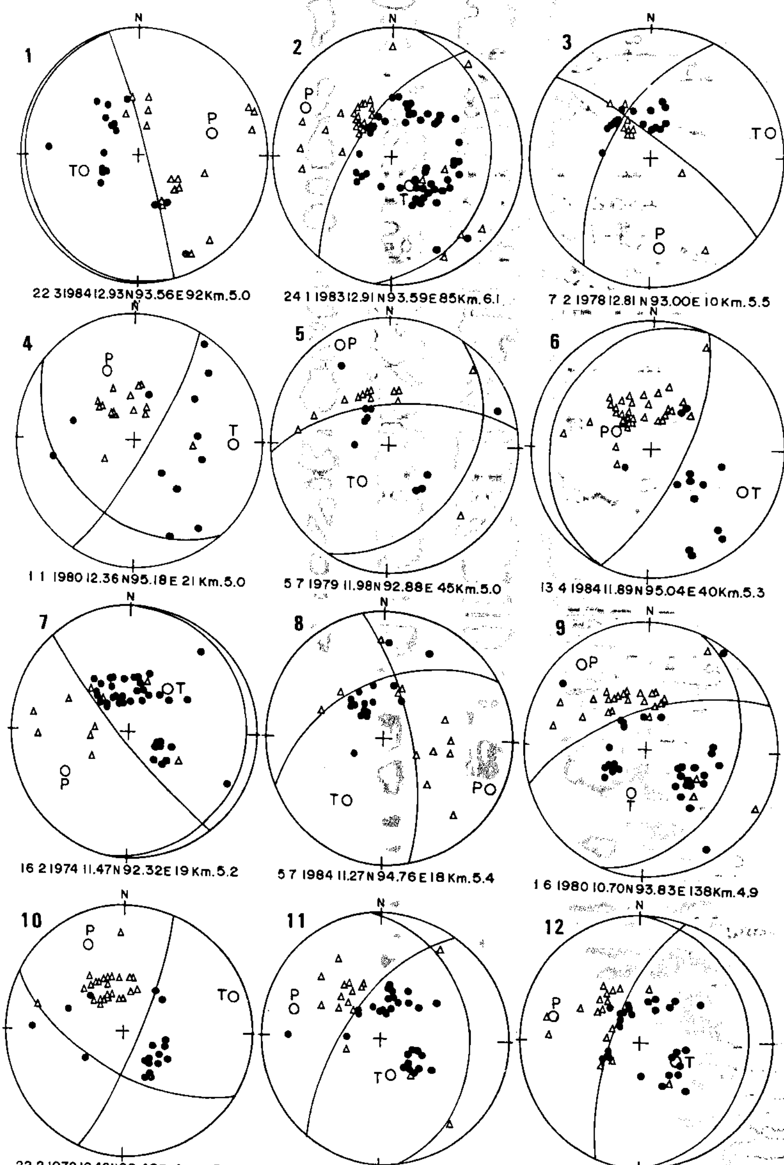

Fig. 4. Lower hemisphere stereographic projection for 47 fault plane solutions of Andaman–Sunda arc earthquakes. ● and △ symbols indicate compressional and dilatational first motion of P waves, respectively. *P* and *T* correspond to the *P*- and *T*-axes. The solution parameters are listed in Table 1.

Cann, 1987) in Sector IV, all of which suggest pure thrusting along a shallow E–NE-dipping nodal plane (< 30°). Except events 2 and 9, all other thrust events are from the upper portion (< 60 km) of the subducting slab. A low incidence of moderate to large interplate thrust earthquakes, particularly in sectors I–III, in comparison to other faulting types (discussed below) possibly indicates a low seismic coupling between the downgoing and overriding plates.

(2) Downdip tensional events along steeply dipping nodal planes (> 60°) and normal faulting along moderately dipping planes (30–45°) are common for the Benioff zone events. Such normal fault mechanism events occur both at the shallow and deeper portions of the Benioff zone. Events 3 and 48 in Sector I, 10, 13, 14 and 16 in Sector II, 22, 23, 34, 37, 39 and 42 in Sector III, and 40, 43 and 44 in Sector IV display normal fault mechanisms in general. Out of the twenty

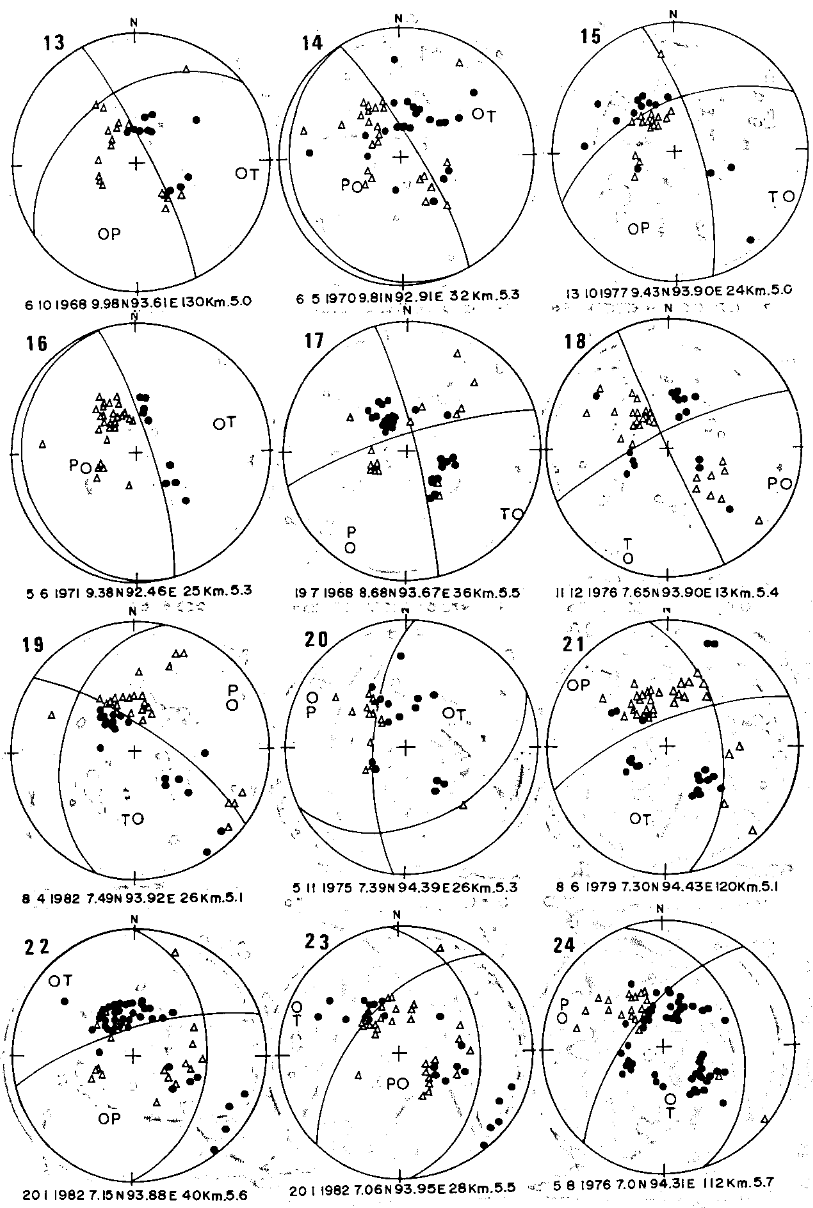

Fig. 4 (continued)

events mentioned above and listed in Table 1, seven are pure downdip tensional type (13, 16, 34, 37, 40, 44 and 48) whereas five events are downdip tensional with a strike-slip component (3, 10, 13, 39 and 43). For the latter category, a dominance of right-lateral shear is evidenced by the solution results (exception is event 10). The remaining three events from Sector III (events 22, 23 and 42) display normal faulting along moderately dipping nodal planes. In sectors I and II, downdip tensional events occur in the shallower part of the Benioff zone, unlike in the Burmese arc further north where thrust type events predominate (Mukhopadhyay and Dasgupta, 1988). In Sector III both downdip tensional and downdip compression earthquakes occur, the latter being the dominant type (see below). Further, many of the downdip tensional events consistently locate along the upper edge of the subducting slab (Fig. 3).

(3) Downdip compression earthquakes illustrating both high-angle reverse fault mechanism (nodal plane > 60°), and reverse faulting along

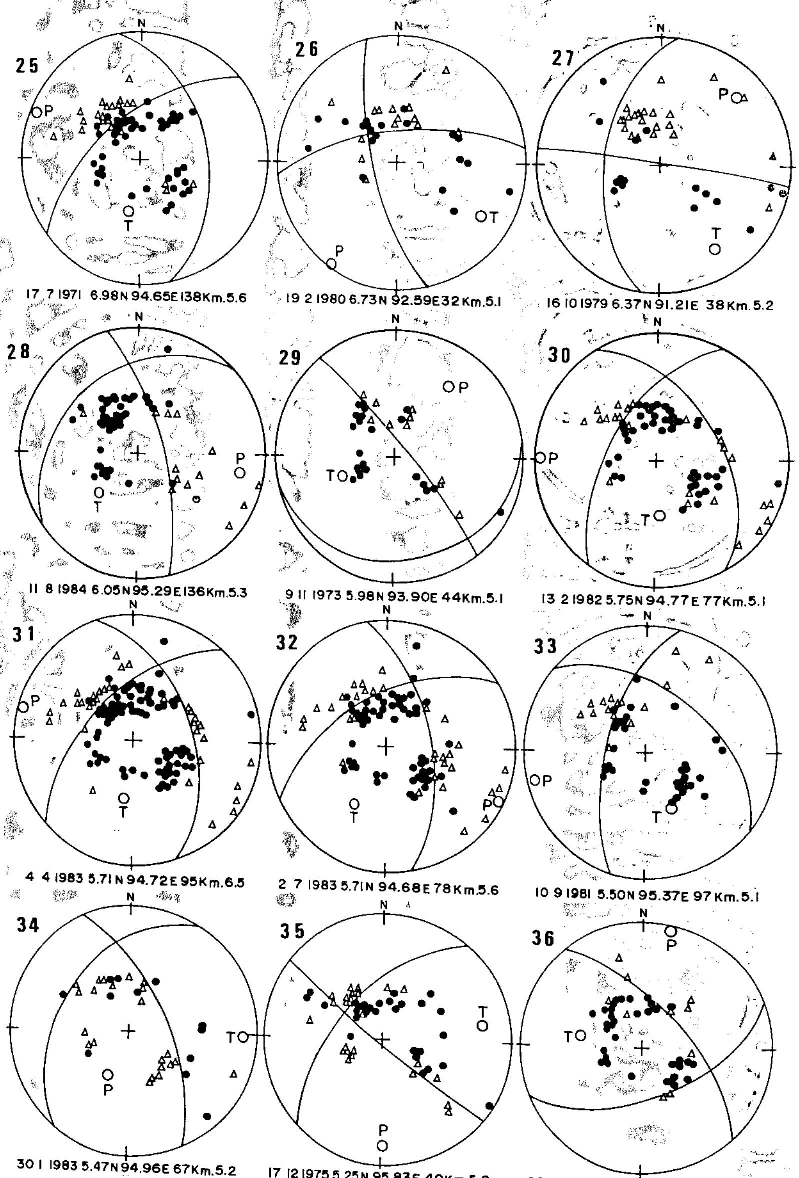

Fig. 4 (continued)

moderately dipping nodal planes (30–45°) occur in sectors I and III. Event 1 in Sector I and events 21, 24, 25, 28–31 and 33 in Sector III are reverse fault type. In Sector I, event 1, is located along the lower edge of the Benioff zone. Also all eight downdip compression events in Sector III (Fig. 3b) locate along the lower edge of the Benioff zone. The presence of a double seismic zone is thus inferred for Sector III where downdip compression events consistently locate along the lower edge and downdip tensional events, mostly along the upper edge (up to ~100 km) within the Benioff zone. The state of stress within the Andaman arc "double seismic zone" is, however, the reverse of what is known from other arcs, for instance, the Tonga arc as reported by Kawakatsu (1986a, b). The latter arc shows downdip compression along the upper edge and downdip tensional along the lower edge of the double seismic zone. This presumably indicates that the double seismic zone within the subducting Indian lithosphere is unrelated to unbending of the slab at

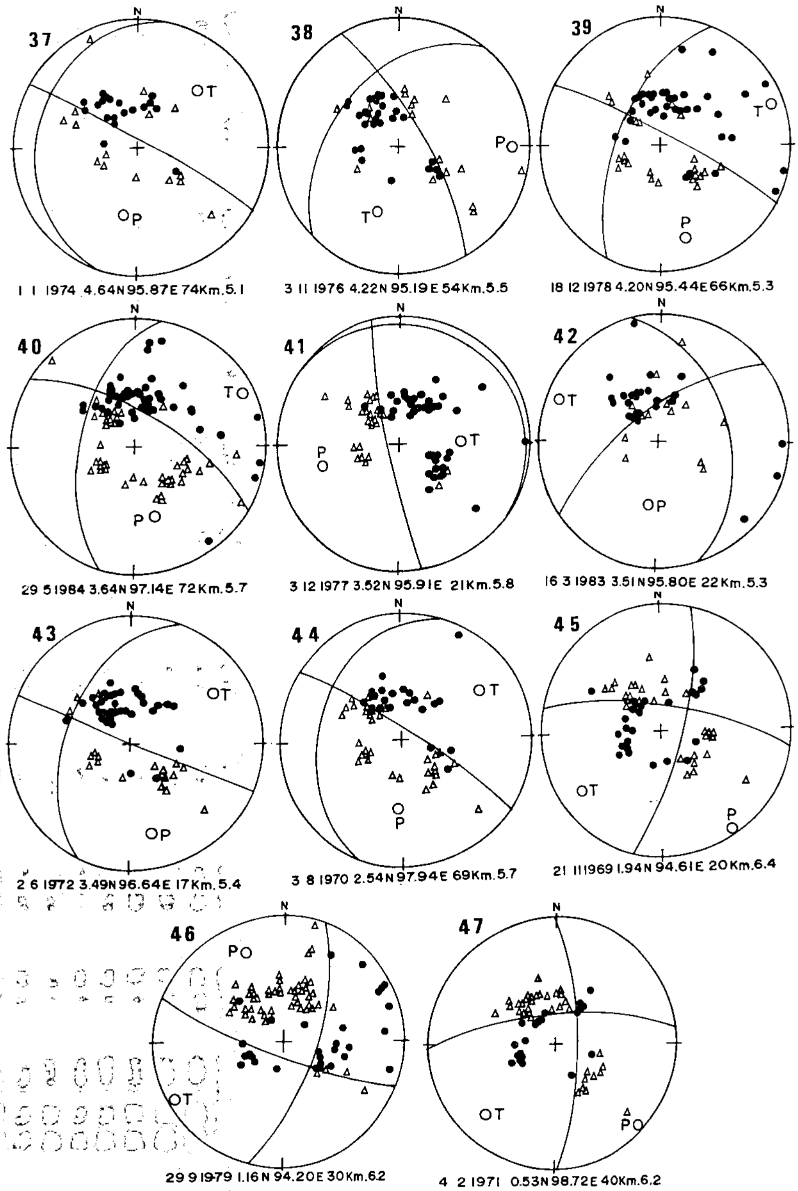

Fig. 4 (continued)

TABLE 1

Parameters of fault plane solutions of earthquakes

No. +	Date	Epicentre		Depth (Km)	Magnitude m_b	P-axis (°)		T-axis (°)		B-axis (°)		Nodal plane 1 (°)			Nodal plane 2 (°)		
		Lat °N	Long °E			PL°	A°$_z$	PL°	A°$_z$	PL°	A°$_z$	S°	D°	Dd°	S°	D°	Dd°
1	22.03.1984	12.93	93.56	92	5.0	41	74	49	254	0	–	N16W	86	74	N16W	4	254
2	24.01.1983	12.91	93.59	85	6.1	20	297	68	148	11	32	N7E	26	97	N36E	66	306
3	07.02.1978	12.81	93.00	10	5.5	31	173	9	77	59	328	N54W	78	36	N28E	62	298
4	01.01.1980	12.36	95.18	21	5.0	41	338	25	91	38	200	N30E	80	120	N48W	40	222
5	05.07.1979	11.98	92.88	45	5.0	14	332	60	216	27	70	N30E	38	120	N83E	64	353
6	13.04.1984	11.89	95.04	40	5.3	65	294	25	114	0	–	N24E	70	114	N42E	20	294
7	16.02.1974	11.47	92.32	19	5.2	38	238	52	42	9	142	N10E	10	100	N40W	84	230
8	05.07.1984	11.27	94.76	18	5.4	11	115	30	212	49	10	N12W	72	78	N62E	54	332
9	01.06.1980	10.70	93.83	138	4.9	28	320	60	196	24	60	N20E	23	110	N68E	67	338
10	22.02.1972	10.42	92.48	4	5.4	28	336	12	70	62	182	N22E	80	112	N64W	64	206
11	21.04.1976	10.29	92.86	52	5.3	27	287	66	157	19	29	N5W	30	85	N35E	66	305
12	05.11.1971	10.11	92.93	53	5.9	25	284	64	120	7	19	N	20	90	N20E	70	290
13	06.10.1968	9.98	93.61	130	5.0	38	206	23	98	42	343	N25W	81	65	N54E	42	324
14	06.05.1970	9.81	92.91	32	5.3	55	240	35	60	0	–	N30W	80	60	N30W	10	240
15	13.10.1977	9.43	93.90	24	5.0	31	211	9	113	56	8	N16W	76	74	N64E	60	334
16	05.06.1971	9.38	92.46	25	5.3	55	240	35	60	0	–	N27W	80	63	N27W	10	243
17	19.07.1968	8.86	93.67	36	5.5	14	211	2	120	78	15	N16W	84	74	N72E	80	342
18	11.12.1976	7.65	93.90	13	5.4	8	108	8	200	80	332	N25W	90	–	N64E	10	334
19	08.04.1982	7.49	93.92	26	5.1	22	64	47	176	36	317	N55W	75	35	N16E	40	286
20	05.01.1975	7.39	94.39	26	5.3	16	296	56	49	32	199	N64E	40	154	N4E	68	274
21	08.06.1979	7.30	94.43	120	5.1	10	302	38	204	52	48	N10W	56	80	N68E	74	338
22	20.01.1982	7.15	93.88	40	5.6	45	206	15	312	40	57	N	44	90	N72E	74	342
23	20.01.1982	7.06	93.95	28	5.5	70	172	12	294	24	28	N4W	40	86	N42E	60	312
24	05.08.1976	7.0	94.31	112	5.7	15	296	56	173	30	27	N20W	40	70	N40E	70	310
25	17.07.1971	6.98	94.65	138	5.6	8	292	54	192	36	29	N10W	48	80	N50E	62	320
26	19.02.1980	6.73	92.59	32	5.1	2	214	28	124	63	312	N82E	70	352	N14W	74	256
27	16.10.1979	6.37	91.21	38	5.2	25	48	26	147	54	280	N83W	88	7	N6E	54	276
28	11.08.1984	6.05	95.29	136	5.3	22	100	53	222	30	356	N12W	74	78	N52E	34	322
29	09.11.1973	5.98	93.90	44	5.1	34	38	52	248	19	139	N39W	82	51	N80E	20	170
30	13.02.1982	5.75	94.77	77	5.1	5	270	54	176	36	5	N32W	50	58	N30E	60	300
31	04.04.1983	5.71	94.72	95	6.5	4	285	51	188	38	18	N18W	52	72	N44E	60	314
32	02.07.1983	5.71	94.68	78	5.6	2	114	46	208	44	22	N10W	62	80	N59E	58	331
33	10.09.1981	5.50	95.37	97	5.1	8	254	51	155	39	352	N51W	50	39	N14E	64	284

34	30.01.1983	5.47	94.96	67	5.2	58	204	12	92	31	352	N22W	66	68	N34E	40	304
35	17.12.1975	5.25	95.83	40	5.6	17	177	23	80	60	302	N53W	86	233	N40E	60	310
36	22.04.1967	5.12	96.39	44	5.4	3	13	48	280	46	108	N44W	64	46	N66E	58	156
37	01.01.1974	4.64	95.87	74	5.1	46	189	39	46	20	300	N61W	86	29	N20E	20	290
38	03.11.1976	4.22	95.19	54	5.5	17	90	37	198	39	344	N30W	74	60	N42E	44	312
39	18.12.1978	4.20	95.44	66	5.3	27	163	12	70	60	314	N66W	80	24	N18E	62	288
40	29.05.1984	3.64	97.14	72	5.7	44	162	12	62	44	324	N60W	69	30	N13E	53	283
41	03.12.1977	3.52	95.91	21	5.8	38	256	52	87	6	348	N54W	8	36	N12W	84	258
42	16.03.1983	3.51	95.80	22	5.3	49	187	13	292	40	36	N18W	45	72	N52E	70	322
43	02.06.1972	3.49	96.64	17	5.4	30	166	30	60	46	290	N78W	90	–	N22E	46	292
44	03.08.1970	2.54	97.94	69	5.7	45	184	30	60	30	308	N56W	82	34	N18E	30	288
45	21.11.1969	1.94	94.61	20	6.4	2	147	21	236	70	56	N78W	74	12	N15E	76	105
46	29.09.1979	1.16	94.20	30	6.2	25	336	5	242	68	137	N70W	80	200	N17E	70	107
47	04.02.1971	0.53	98.72	40	6.2	2	132	24	223	68	32	N2W	76	88	N84E	72	354
48	06.09.1967	14.65	93.55	36	5.5	59	286	31	106	0	–	N16E	76	106	N16E	15	286
49	28.07.1964	14.17	96.12	22	5.9	71	45	7	160	16	250	N80E	56	170	N52E	40	322
50	14.02.1967	13.75	96.47	13	5.6	80	330	10	150	0	–	N60E	55	150	N60E	35	330
51	12.08.1971	12.50	95.08	20	5.3	13	34	12	300	73	174	N12W	88	258	N78E	73	168
52	13.11.1972	12.20	95.30	33	5.4	12	30	4	297	77	182	N16W	86	254	N74E	76	164
53	28.03.1971	12.12	95.22	22	5.2	2	45	2	315	87	180	N	90	–	N90E	87	180
54	29.03.1971	11.16	95.11	17	5.1	1	236	15	144	75	327	N8E	81	278	N80W	79	10
55	09.07.1973	10.66	92.59	44	5.6	12	182	22	86	63	305	N45W	86	225	N47E	65	313
56	15.09.1964	8.9	93.03	89	6.3	17	204	52	88	34	308	N39W	70	231	N78E	38	348
57	02.07.1967	8.65	93.59	44	5.7	10	215	10	307	76	81	N9W	75	81	N81E	90	–
58	30.11.1964	6.75	94.54	24	5.7	0	–	0	–	90	–	N34W	90	–	N56E	90	–
59	02.04.1964	5.75	95.42	65	5.6	3	196	3	285	86	60	N30W	86	60	N60E	90	
60	12.04.1967	5.32	96.45	45	5.4	17	8	73	188	0	–	N82W	28	188	N82W	62	8
61	15.06.1964	5.28	96.82	46	5.3	11	16	65	264	36	102	N56W	60	36	N64E	51	154
62	03.04.1964	3.91	96.56	51	5.8	65	200	26	20	0	–	N70W	70	20	N70W	20	200
63	21.08.1967	3.72	95.74	40	6.1	33	203	57	23	0	–	N67W	12	23	N67W	78	203
64	07.04.1973	7.00	91.32	39	5.8	10	350	1	78	82	168	N34E	84	124	N56W	86	214
L3	30.10.1976	3.52	96.34	29	5.5	–	–	–	–	–	–	–	–	–	–	–	–
L4	20.06.1976	3.40	96.28	11	6.3	–	–	–	–	–	–	–	–	–	–	–	–
L5	21.06.1976	3.43	96.42	5	5.7	–	–	–	–	–	–	–	–	–	–	–	–
L7	04.12.1974	0.50	97.89	20	5.8	–	–	–	–	–	–	–	–	–	–	–	–

Nos. 1–47, present study; 48–50, 56, Fitch, (1970) (50 reinterpreted by Eguchi et al., 1979); 51–57, Eguchi et al. (1979); 57, 58–63, Fitch (1972); 64, Bergman and Solomon (1985); L3–L5, L7, Newcomb and McCann (1987).

PL = plunge; Az = azimuth; S = strike; D = dip; Dd = dip direction.

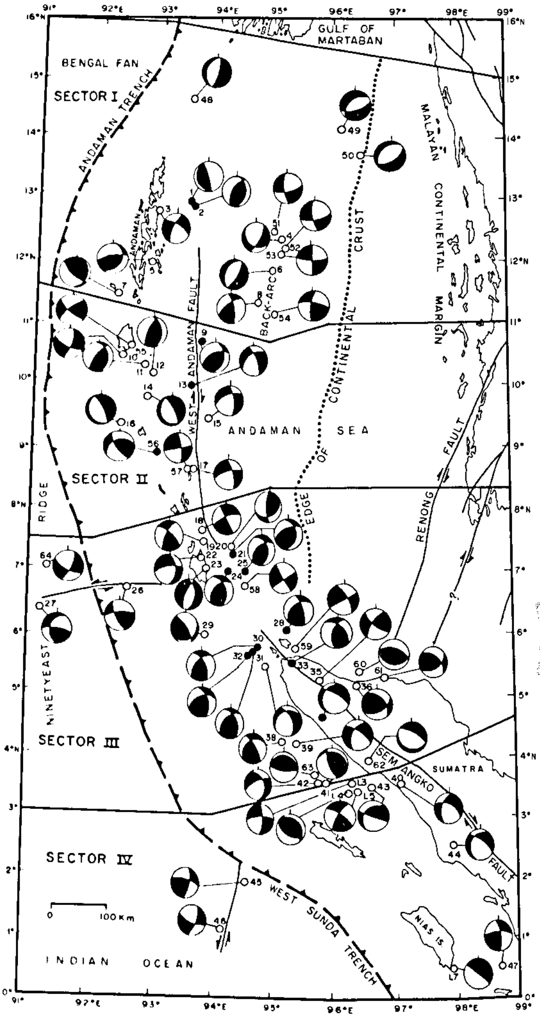

Fig. 5. Results of 68 focal mechanism solutions for the Andaman–Sunda arcs are shown schematically. Dark and blank areas refer to compressional and dilatational quadrants, respectively. Digits identify the solution number as listed in Table 1. Diverging arrows indicate lateral slip. Sectors I to IV are the same as illustrated in Fig. 2.

intermediate depths (see House and Jacob, 1983); rather the bending strain prevails even at intermediate depths within the subducting plate, resulting in the production of downdip tensional events along the upper edge and downdip compression events below it.

(4) Events 26 and 27 in Sector III, along with few other earthquake epicentres presumably define a transverse seismic zone across the Andaman trench. The suggested fault location between 6 and 7°N latitudes is also identifiable from the relief contour map (Bathymetric Chart of Bay of Bengal, Naval Hydrographic Office, 1974, Dehra Dun, India), and may be correlated with a wide ridge/upper trench slope in the southern Andaman Sea (Moore et al., 1980). Focal mechanism solutions for both events suggest left lateral shear along a E–W fault (Fig. 4). Events 55 (after Eguchi et al., 1979) and 56 (after Fitch, 1970) in Sector II display similar focal mechanism solutions where both the nodal planes orient transverse to the Andaman arc.

(5) Events 45, 46 in Sector IV indicate left-lateral shear seaward of the West Sunda trench (Figs. 4 and 5). Some support to this inference is given by magnetic anomaly interpretations in the northeastern Indian Ocean (cf. Royer and Sandwell, 1989). For event 64, Bergman and Solomon (1985) assigned the NNE nodal plane as the fault plane and correlated it with left-lateral slip at the east margin of the Ninetyeast Ridge. Earthquakes L3, L5 (after Newcomb and McCann, 1987) and 47 all from Sector IV further indicate left-lateral shear along nodal planes subparallel to the arc.

Summary and concluding remarks

In the northern Andaman Sea (Sector I), shallow-focus earthquakes occur only in the back-arc areas (Figs. 2 and 3a); whereas in the southern Andaman Sea (sectors II and III) the back-arc area is aseismic and shallow-focus upper plate earthquakes are restricted to the fore-arc domain. In Sector I earthquakes define a NNE linear zone (Fig. 2). Focal mechanism solutions from this seismic zone indicate normal and strike-slip faulting where active back-arc spreading in E–W direction is inferred (Curray et al., 1979; Eguchi et al., 1979). In section I (Fig. 3) seismicity is concentrated in a narrow zone east of the Alcock Seamount. Four hypocentral sections drawn traversing the Andaman–West Sunda arc reveal significant variations in the geometry of the Benioff zone in a N–S direction. Available data demonstrate that a somewhat contorted Benioff zone outlines the deeper lithosphere (~ 100–170 km depths) in the southern Andaman and northernmost Sumatra region. Approximately here, the Ninetyeast Ridge also impinges on the Andaman subduction zone on the oceanward side. While the details of the inferred "Contorted Benioff Zone" are unclear at the moment, it offers an interesting possibility that the Malayan continental margin may be locally deformed and involved in the subduction process below the southern Andaman Sea. In terms of hypocentral distribution, stress pattern and fault geometry (refer text), this region has at least certain conceptual analogy with the Hindukush–Pamir contorted Benioff zone (cf. Billington et al., 1977) where tectonic processes have however reached the final stages of subduction.

An interesting feature of earthquakes originating in the Andaman Sea is the position of the shallow seismic zone with respect to the magmatic arc. While in Sector I this zone locates to the continental side of the arc, it occupies the fore-arc position in Sector II, thereby constraining the position of the aseismic belt in section as illustrated in Figure 3a. On map view, the earthquakes are located between the Nicobar Deep and the Sewell Seamount and mostly display lateral movement along N–S nodal planes correlatable with the West Andaman fault.

Solutions 4, 6, 49 and 50 indicate normal faulting along NNE-trending, steeply dipping nodal planes, while events 51–54 give strike-slip solution correlatable to short transforms in the back-arc seismic zone (see Fig. 1). The only exception to this trend is provided by the solution for event 8 from the southern part of Sector I that shows reverse faulting with lateral slip. Dziewonski et al. (1983) gave eleven solutions from this back-arc seismic zone for events of an earthquake swarm that occurred between July 8 and 23, 1984. Swarms of such low-magnitude earthquakes at spreading centres are probably associated with magmatic intrusions in the rift valley. All centroid moment tensor solutions give normal fault mechanisms with or without strike-slip component; such normal faulting events occur on the flanks of the crest, driven by isostatic uplift of the depressed central rift valley (cf. Scholz, 1990). Centroid moment tensor depths for earthquakes in the northern Andaman Sea varies between 10 and 25 km which indicate that rifting penetrates at best twice the centroid moment tensor depth, i.e., of the order of 50 km. In Sector III events 60 and 61 (both after Fitch, 1972) are located just north of the Sumatra magmatic arc (Fig. 5) and presumably indicate back-arc thrust environment as in the East Sunda arc (Silver et al., 1983).

Solutions 17 and 57 (after Fitch, 1972) suggest right-lateral movement along N–S planes, while event 15 displays normal fault mechanism with right lateral slip. Events 18–20 in Sector III possibly relate to the activity of the West Andaman fault, and suggest right-lateral slip. A compressive stress field dominates the fore-arc as revealed by a number of solutions showing high angle reverse faulting. Events 35, 36, 58, 59 and 62 in Sector III are fore-arc earthquakes that display right-lateral slip related to the Semangko fault or its northern continuation. Solution 62 located further south of the Semangko fault however indicates normal fauling. The above analysis of seismicity and stress distribution in the subducting lithosphere as well as in the overriding plate suggests that the interplate coupling clearly changes from north to south resulting in an overall tensional stress regime in the northern Andaman Sea that gradually becomes compressive in southern Andaman and northern Sumatra.

Acknowledgement

Shri N. Karmakar drafted the figures.

References

Bergman, E.A. and Solomon, S.C., 1985. Earthquake source mechanisms from body-waveform inversion and intraplate tectonics in the northern Indian Ocean. Phys. Earth Planet. Inter., 40: 1–23.

Billington, S., Isacks, B. and Barazangi, M., 1977. Spatial distribution and focal mechanisms of mantle earthquakes in the Hindkush–Pamir region: A contorted Benioff zone. Geology, 5: 699–704.

Closs, H., Narain, H. and Garde, S.C., 1974. Continental margins of India. In: C.A. Burk and C.L. Drake (Editors), The Geology of Continental Margins. Springer, New York, NY, pp. 629–639.

Curray, J.R., 1987. The Sunda Arc: A model for oblique plate convergence. In: J.E. Van Hinte, Tj. C-E. van Weering and A.R. Fortruin (Editors), Proc. Symp. Snellius-II Expedition, Jakarta, Nov. 23-28, 1987. Vol. I. Geology and Geophysics of the Banda Arc and Adjacent Areas. Neth. J. Sea Res. (preprint).

Curray, J.R., Moore, D.G., Lawver, L.A., Emmel, F.J., Raitt, R.W., Henry, M. and Kieckhefer, R., 1979. Tectonics of the Andaman Sea and Burma. Am. Assoc. Pet. Geol. Mem., 29: 189-198.

Curray, J.R., Emmel, F.J., Moore, D.G. and Raitt, R.W., 1982. Structure, tectonics and geological history of the North-eastern Indian Ocean. In: A.E.M. Nairn and F.G. Stehli (Editors), The Ocean Basins and Margins. Plenum, New York, NY, Vol. 6, pp. 399-450.

Dziewonski, A.M., Friedman, A., Giardini, D. and Woodhouse, J.H., 1983. Global seismicity of 1982: Centroid-moment tremor solutions for 308 earthquakes. Phys. Earth Planet. Inter., 33: 76-90.

Eguchi, T., Uyeda, S. and Maki, T., 1979. Seismotectonics and tectonic history of the Andaman Sea. Tectonophysics, 57: 35-51.

Fitch, T.J., 1970. Earthquakes mechanisms in the Himalaya, Burmese, and Andaman regions and continental tectonics in central Asia. J. Geophys. Res., 75: 2699-2709.

Fitch, T.J., 1972. Plate convergence, transcurrent faults, and internal deformation adjacent to Southeast Asia and the Western Pacific. J. Geophys. Res., 77: 4432-4460.

Hamilton, W.B., 1979. Tectonics of the Indonesian region. U.S. Geol. Surv., Prof. Pap. 1078, 345 pp.

House, L.S. and Jacob, K.H., 1983. Earthquakes, plate subduction and stress reversals in the Eastern Aleutian arc. J. Geophys. Res., 88(B11): 9347-9373.

Kawakatsu, H., 1986a. Double seismic zones: Kinematics. J. Geophys. Res., 91(B5): 4811-4825.

Kawakatsu, H., 1986b. Downdip tensional earthquakes beneath the Tonga arc: A double seismic zone. J. Geophys. Res., 91(B6): 6432-6440.

Maung, H., 1987. Transcurrent movements in the Burma-Andaman Sea region. Geology, 15: 911-912.

Moore, G.F. and Curray, J.R., 1980. Structure of the Sunda trench lower slope off Sumatra from multichannel seismic reflection data. Mar. Geophys. Res., 4: 319-340.

Moore, G.F. and Karig, D.E., 1980. Structural geology of Nias Island, Indonesia: Implications for subduction zone tectonics. Am. J. Seismol., 280: 193-223.

Moore, G.F. and Curray, J.R., Moore, D.G. and Karig, D.E., 1980. Variations in geologic structure along the Sunda forearc, NE Indian Ocean. In: D.E. Hayes (Editor), The Tectonics and Geologic Evolution of SE Asian Seas and Islands. Am. Geophys. Union, Monogr., 23: 145-160.

Mukhopadhyay, M., 1984. Seismotectonics of subduction and backarc rifting under the Andaman Sea. Tectonophysics, 108: 229-239.

Mukhopadhyay, M., 1988. Gravity anomalies and deep structure of the Andaman arc. Mar. Geophys. Res., 9: 197-210.

Mukhopadhyay, M. and Dasgupta, S., 1988. Deep structure and tectonics of the Burmese arc: Constraints from earthquake and gravity data. Tectonophysics, 149: 299-322.

Mukhopadhyay, M. and Krishna, M.R., 1991. Gravity field and deep structure of the Bengal Fan and its surrounding continental margins, northeast Indian Ocean. Tectonophysics, 186: 365-386.

Newcomb, K.R. and McCann, W.R., 1987. Seismic history and seismotectonics of the Sunda arc. J. Geophys. Res., 92(B1): 421-439.

Rodolfo, K.S., 1969. Bathymetry and marine geology of the Andaman basin and tectonic implications for SE Asia. Am. Assoc. Pet. Geol. Bull., 52: 2422-2437.

Royer, J.-Y. and Sandwell, D.T., 1989. Evolution of the eastern Indian Ocean since the late Cretaceous: Constraints from Geosat altimetry. J. Geophys. Res., 94: 13,755-13,782.

Scholz, C.N., 1990. The Mechanics of Earthquakes and Faulting. Cambridge Univ. Press, Cambridge, 435 pp.

Silver, E.A., Donald, R. and McCaffrey, R., 1983. Backarc thrusting in the eastern Sunda arc, Indonesia: A convergence of arc-continent collision. J. Geophys. Res., 88(B9): 7429-7448.

Uyeda, S. and Kanamori, H., 1979. Back-arc opening and the mode of subduction. J. Geophys. Res., 84: 1049-1061.

Weeks, L.A., Harbison, R.A. and Peter, G., 1967. Island arc system in Andaman Sea. Am. Assoc. Pet. Geol. Bull., 51: 1803-1815.